NATIONAL ADVISORY COMMITTEE FOR AERONAUTICS

TECHNICAL NOTE 3661

SELF SHIELDING IN RECTANGULAR AND CYLINDRICAL GEOMETRIES

By Harold Schneider, Paul G. Saper, and Charles F. Kadow

Lewis Flight Propulsion Laboratory
Cleveland, Ohio

Washington
April 1956

NATIONAL ADVISORY COMMITTEE FOR AERONAUTICS

TECHNICAL NOTE 3661

SELF SHIELDING IN RECTANGULAR AND CYLINDRICAL GEOMETRIES

By Harold Schneider, Paul G. Saper, and Charles F. Kadow

SUMMARY

The steady-state diffusion P_2 and transport theory P_3 solutions of several self-shielding problems have been obtained for multiregion cells of rectangular and cylindrical geometries. These cells represent a given arrangement of moderator, fuel, and cladding; usually considered to be homogeneous. The three-region cells studied were of slab geometry only and consisted of water, steel, and uranium regions. The two-region cells were of identical volumetric proportions and compositions, differing only in the homogeneous dispersion of uranium in water. The dimensions of the equivalent two regions of the cylindrical cell were chosen so that the same homogeneous self-shielding factor of the corresponding slab cell was maintained. Additional results were calculated considering the effects of the chemical binding in water on the flux distributions and self-shielding factors.

The neutrons were assumed to be monoenergetic; their distribution function assumed to be dependent on but one spatial coordinate, and the scattering in the center of mass system assumed to be spherically symmetrical. The P_2 approximation underestimated the magnitude of self-shielding effects relative to the P_3 approximation for all cases. Consideration of chemical binding in water was unimportant in calculating self-shielding factors for the three-region cell but could not be neglected for the two-region cell where the water and fuel were homogeneously mixed. An electromechanical differential analyzer was used to solve the P_2 and P_3 flux equations.

INTRODUCTION

In zero power criticality experiments, it is usual to mock up the reactor composition in the most expedient way. A fuel-element moderator assembly may be represented by fuel strips temporarily attached to plates of cladding material or by solutions of enriched uranium salt in liquid moderator. In analyzing these criticality experiments, it is important to know how a given fuel-element moderator assembly departs

from the homogeneous conditions. Inasmuch as the dimensions of repetitive cells in an assembly are generally very much less than the average mean free path, solutions of higher order than diffusion theory are required to evaluate departures from homogeneity.

The steady-state diffusion-theory solutions and the next higher order approximation of several self-shielding problems have been obtained for multiregion cells of rectangular and cylindrical geometry. The neutrons have been assumed to be monoenergetic, and their distribution function has been assumed to be dependent on but one spatial coordinate. Spherically symmetrical scattering in the center of mass system has also been assumed. The solutions of the diffusion theory P_2 and the transport theory P_3 flux equations were obtained by a differential analyzer. (All symbols used herein are defined in appendix A.)

The cases studied for rectangular geometry were (a) a three-region cell consisting of water, steel, and uranium, and (b) a two-region cell consisting of identical volumetric proportions and compositions except for the homogeneous dispersion of uranium in water. The case studied for cylindrical geometry was a two-region cell having the same homogeneous self-shielding factor as that of case (b).

Additional results were obtained by approximating the effects of molecular binding in the water molecule by a method derived by A. Radkowsky in a classified publication. The thermal neutron flux distributions were used to compute the ratio R of total absorption in uranium to the total absorption in the cell.

The detailed derivation of the flux equations in the P_3 approximation in rectangular geometry is given in reference 1. The equations for the P_3 approximation of cylindrical geometry are derived in detail in appendix B. These equations were also obtained by R. R. Haeffner in a somewhat different manner and presented in a classified publication.

ANALYSIS

Neutron Flux Equations and Boundary Conditions

For Three-Region Slab Cell

Assuming a constant isotropic source of thermal neutrons S_A for water region A, the P_3 approximation for this region leads to the equations (ref. 1)

$$\left.\begin{aligned} F_1'(x) + a_0F_0(x) - S_A &= 0 \\ F_0'(x) + 2F_2'(x) + 3a_1F_1(x) &= 0 \\ 2F_1'(x) + 3F_3'(x) + 5a_2F_2(x) &= 0 \\ 3F_2'(x) + 7a_3F_3(x) &= 0 \end{aligned}\right\} \tag{1}$$

where F_k is the k^{th} ($k = 0, 1, 2, 3$) coefficient of the Legendre expansion of the flux function. Physically, F_0 is the total neutron flux and F_1 is the net neutron current. The coefficients denoted by a_k ($k=0,1,2,3$) are given by

$$a_k = \Sigma^A - N_S^A\sigma_{S,k}^A$$

where N_S^A is the number of scattering nuclei per cubic centimeter of region A, Σ is the total macroscopic cross section, and $\sigma_{S,k}$ is the k^{th} coefficient of the Legendre expansion of the scattering function. The values of $\sigma_{S,k}$ are calculated for spherically symmetric scattering in the center of mass system in appendix C. The value of S_A is taken as 1 neutron per cubic centimeter per second. Identical sets of equations hold in regions B and C with the term a replaced by b and c, respectively, and with a zero source in these regions.

Eliminating F_1 and F_3 from equations (1) and formally integrating with respect to x

$$\left.\begin{aligned} -\frac{1}{3a_1}F_0' + a_0\int F_0dx &= x + \frac{2}{3a_1}F_2' \\ -\left(\frac{4}{15a_1} + \frac{9}{35a_3}\right)F_2' + a_2\int F_2dx &= \frac{2}{15a_1}F_0' \end{aligned}\right\} \tag{2}$$

with a similar set of equations in regions B and C. The equations in this form are suitable for solution by a differential analyzer.

The boundary conditions are

$$\left.\begin{aligned} F_0'(0) &= 0 \\ F_2'(0) &= 0 \\ F_0'(\gamma) &= 0 \\ F_2'(\gamma) &= 0 \end{aligned}\right\} \quad \text{at the extreme boundaries } 0 \text{ and } \gamma \qquad \begin{matrix} (3a) \\ (3b) \\ (3c) \\ (3d) \end{matrix}$$

$$\left.\begin{aligned} F_{0,A}(\alpha) &= F_{0,B}(\alpha) \qquad (4a) \\ F_{2,A}(\alpha) &= F_{2,B}(\alpha) \qquad (4b) \\ \frac{F_{0,A}'(\alpha) + 2F_{2,A}'(\alpha)}{a_1} &= \frac{F_{0,B}'(\alpha) + 2F_{2,B}'(\alpha)}{b_1} \qquad (4c) \\ \frac{F_{2,A}'(\alpha)}{a_3} &= \frac{F_{2,B}'(\alpha)}{b_3} \qquad (4d) \end{aligned}\right\} \quad \text{at boundary } \alpha$$

$$\left.\begin{aligned} F_{0,B}(\beta) &= F_{0,C}(\beta) \qquad (5a) \\ F_{2,B}(\beta) &= F_{2,C}(\beta) \qquad (5b) \\ \frac{F_{0,B}'(\beta) + 2F_{2,B}'(\beta)}{b_1} &= \frac{F_{0,C}'(\beta) + 2F_{2,C}'(\beta)}{c_1} \qquad (5c) \\ \frac{F_{2,B}'(\alpha)}{b_3} &= \frac{F_{2,C}'(\beta)}{c_3} \qquad (5d) \end{aligned}\right\} \quad \text{at boundary } \beta$$

Equations (4) and (5) follow from continuity requirements on the $F_{k,s}$ at the interfaces α and β whereas equations (3) follow from the requirement that F_1 and F_3 vanish at 0 and γ (ref. 1).

By setting $F_2 \equiv 0$, equations (2) to (5) reduce to diffusion theory with the diffusion and absorption coefficients being given by $D = \frac{1}{3a_1}$ and a_0, respectively. The specialization of equations (2) to (5) to two-region cases follows directly.

Specific slab configurations. - Figure 1 shows the rectangular cells studied and gives the specific dimensions used. The neutron cross sections are given in figure 2. The volume proportions of the repeated slab array used were steel:fuel:steel:water, 26.7:1:26.7:52.3 leading to symmetrical cell volume proportions of fuel:steel:water, 0.50:26.7:26.15. The specific solutions obtained correspond to an enriched fuel thickness of 3 mils (1.5 mils in the cell).

The dimensions and nuclear constants listed in figures 1 and 2 and the values of $\sigma_{S,k}$ computed in appendix C were used to calculate the coefficients which were substituted into equations (2) to (5). For greater accuracy and convenience the strongly absorptive uranium region ($\Sigma_a = 33$) was magnified 20 times by means of a linear transformation of the independent variable.

Results for the chemically bound cases were obtained by the use of an effective hydrogen mass M and an average hydrogen transport cross section $\overline{\sigma}_{tr}^{H}$, the latter having been derived by A. Radkowsky in order to approximate the effects of chemical binding of the hydrogen. The quantity M is defined by

$$\overline{\sigma}_{tr}^{H} = \overline{\sigma}_{S}^{H}\left(1 - \frac{2}{3M}\right)$$

where $\overline{\sigma}_{S}^{H}$ is the average hydrogen scattering cross section averaged over a Maxwellian distribution of neutron flux.

The values of M, $\overline{\sigma}_{tr}^{H}$, and $\overline{\sigma}_{S}^{H}$ for water at room temperature are 2.0, 31.4, and 46.7, respectively. For the unbound case, M was taken as 1, and σ_{S}^{H} as 25.6 barns from which it follows that $\sigma_{tr}^{H} = 8.55$ barns.

From the flux distributions, the self-shielding factors R were calculated by

$$R = \frac{\text{total absorption by uranium}}{\text{total absorption in cell}}$$

$$= \frac{\int_{\text{uranium}} F_0^U(x)\Sigma_a^U\,dx}{\int_{\text{uranium}} F_0^U(x)\Sigma_a^U dx + \int_{\text{steel}} F_0^{\text{steel}}(x)\Sigma_a^{\text{steel}}dx}$$

$$= \frac{\overline{F}_0{}^U\Sigma_a^U V^U}{\overline{F}_0{}^U\Sigma_a^U V^U + \overline{F}_0{}^{\text{steel}}\Sigma_a^{\text{steel}} V^{\text{steel}}}$$

where $\overline{F}_0^{\text{steel}}$ is the average flux in steel, V^U is the volume of the uranium region. The absorption in water is neglected since $\Sigma_a^{H_2O}$ is negligible.

The magnitude of self-shielding effects may be measured by deviations in R from the value of $R_H = 0.712$ calculated for the case of a constant flux throughout the cell, that is, $\overline{F}_0^U = \overline{F}_0^S$, which is equivalent to assuming that all of the constituents of the cell are homogeneously mixed.

Analyzer procedure for slab solutions. - Equations (2) subject to the boundary conditions of equations (3) to (5) are solved by the differential analyzer in the following manner:

The diffusion P_2 approximation results by setting $F_2(x) \equiv 0$. From the boundary conditions, $F_0'(0)$ must be zero. Since $F_0(0)$ is unknown, it must be guessed in order to begin the solution at the boundary 0. Using the initial $F_0(0)$, the analyzer integrates the F_0 equation until the interface α is reached. At the interface, F_0 is continuous. The discontinuous change of slope $F_{0,B}'(\alpha)$ that must be applied to initiate the solution for region B is calculated by equation 4(c) with $F_2' \equiv 0$. The F_0 equation of region B is then integrated until the interface β is reached where the discontinuous change of slope $F_{0,C}'(\beta)$ necessary to start the solution in region C is calculated by equation 5(c) with $F_2' \equiv 0$. The analyzer then proceeds to integrate the equations of region C until the outer boundary γ is reached. If $F_0'(\gamma)$ turns out 0, then the correct $F_0(0)$ has been guessed. If $F_0'(\gamma) \neq 0$, then another value $F_0(0)$ is guessed until this criterion is satisfied. The final results are shown graphically in figure 2.

After obtaining the diffusion answer, equations (2) were set up to be solved simultaneously. For the first trial, the diffusion theory $F_0(0)$ was used, and an initial value of $F_2(0)$ was guessed. The conditions of equations (4) and (5) were used to compute the discontinuous changes in the slope at the interfaces. Thereafter, both $F_0(0)$ and $F_2(0)$ were guessed simultaneously until the conditions $F_0'(\gamma) = 0$ and $F_2'(\gamma) = 0$ were met. The total operating time for convergence turned out to be 8 to 16 hours for a two-region cell and 16 to 32 hours for a three-region cell.

Equivalent Two-Region Cylindrical Cell

As shown in figure 3, the radii of the two-region cylindrical cell were chosen such that the volume of water plus uranium and the volume of steel were equal to those in a square cylindrical cell formed from the dimensions used in the previous two-region slab cell. With an outer square boundary, the neutron flux will be spatially dependent on an azimuthal angle in the cross section of the cylinder in addition to radial dependence. This angular dependence is not present when the outer square boundary is approximated by a circular one.

From figure 3, the volume of steel per unit depth for the rectangular cell is 0.32773 cubic centimeters, and the volume of water plus uranium is 0.32098 cubic centimeters for a total cell volume of 0.64871 cubic centimeters. This means that for the cylindrical cell

$$\pi a^2 = 0.32773$$

or

$$a = 0.3230 \text{ cm}$$

which is the radius of the steel region, and

$$\pi b^2 = 0.64871$$

$$b = 0.4544 \text{ cm}$$

the radius of the cell. The self-shielding factor R_H then remains the same as in the slab cell (0.712) for the case of a constant flux throughout the cell.

The cylinders are assumed to be infinitely long and the transport flux depends spatially on the radial distance r from the z-axis, and on two angular coordinates α and ξ that determine the direction of the neutron velocity vector (see fig. 4). The azimuthal angle α of the velocity vector is measured from any fixed radial line in the cross section of the cylinder. The polar angle ξ of the velocity vector is measured from the z-axis. The transport flux can be written as $F(r,\mu,\alpha)$ where $\mu = \cos \xi$.

In appendix B, the transport flux is expanded in spherical harmonics to give

$$F(r,\mu,\alpha) = \sum_{n=0}^{\infty} \sum_{m=0}^{\infty} \frac{(n-m)!}{(n+m)!} \frac{2n+1}{2} F_{m,n}(r) \cos m\alpha \, P_n^m(\mu) \qquad \text{(B8)}$$

From the orthogonality of spherical harmonics,

$$\left(2\pi\delta_{j,0} + \pi\delta_{j\neq 0}\right)F_{j,k}(r) = \int_{-\pi}^{\pi}\int_{-1}^{1} F(r,\mu,\alpha)\cos j\alpha\, P_k^{(j)}(\mu)\,d\mu\,d\alpha$$

where the δ's are defined as

$$\delta_{m,s} \equiv \begin{cases} 0 & m \neq s \\ 1 & m = s \end{cases} \qquad \text{and} \qquad \delta_{m\neq s} \equiv \begin{cases} 1 & m \neq s \\ 0 & m = s \end{cases}$$

When $j=k=0$, the right hand side is the transport flux integrated over all directions. This is the total flux $\Phi_{0,0}(r)$. Hence $\Phi_{0,0}(r) = 2\pi F_{0,0}(r)$. With $j=k=1$, the right side is the projection of the vector flux $F(r,\mu,\alpha)$ on the radial axis integrated over all directions and is, therefore, the net neutron diffusion current $\Phi_{1,1}(r)$. Thus, $\Phi_{1,1}(r) = \pi F_{1,1}(r)$.

Assuming a constant isotropic source of neutrons in each volume element of the water-uranium region, in the P_3 approximation (see appendix B), the following set of equations is obtained:

$$F'_{1,1} + \frac{F_{1,1}}{r} + 2b_0F_{0,0} = 2S_{0,0} \tag{B9a}$$

$$F'_{1,3} + \frac{F_{1,3}}{r} - F'_{1,1} - \frac{F_{1,1}}{r} + 10b_2F_{0,2} = 0 \tag{B9b}$$

$$2F'_{0,0} - 2F'_{0,2} + \frac{1}{2}F'_{2,2} + \frac{F_{2,2}}{r} + 3b_1F_{1,1} = 0 \tag{B9c}$$

$$12F'_{0,2} - \frac{1}{2}F'_{2,2} - \frac{F_{2,2}}{r} + 7b_3F_{1,3} = 0 \tag{B9d}$$

$$F'_{3,3} + 3\frac{F_{3,3}}{r} + 12\left(F'_{1,1} - \frac{F_{1,1}}{r}\right) - 2\left(F'_{1,3} - \frac{F_{1,3}}{r}\right) + 10b_2F_{2,2} = 0 \tag{B9e}$$

$$15\left(F'_{2,2} - 2\frac{F_{2,2}}{r}\right) + 7b_3F_{3,3} = 0 \tag{B9f}$$

where b is defined in terms of nuclear constants by

$$b_k = N\sigma - N_S\sigma_{S,k} \qquad k = 0,1,2,3$$

Transforming to fluxes $\Phi_{j,k}$ and the neutron source $s_{0,0}$ by

$$\Phi_{0,k} = 2\pi F_{0,k} \qquad k = 0,2$$

$$\Phi_{j,k} = \pi F_{j,k} \qquad j = 1,2,3 \qquad k = 1,2,3$$

$$s_{0,0} = 2\pi S_{0,0}$$

and after eliminating $F_{1,1}$, $F_{1,3}$, and $F_{3,3}$ from equations (B9) and formally integrating with respect to r yields

$$\left.\begin{aligned}
&-\frac{1}{3b_1}\left[\Phi'_{0,0}+\int\frac{d\Phi_{0,0}}{r}\right]+b_0\int\Phi_{0,0}\,dr = s_{0,0}\,r+\frac{1}{3b_1}\left[-\Phi'_{0,2}-\int\frac{d\Phi_{0,2}}{r}+\frac{\Phi'_{2,2}}{2}+\frac{3}{2}\int\frac{d\Phi_{2,2}}{r}\right]\\
&-\frac{6}{7b_3}\left[\Phi'_{0,2}+\int\frac{d\Phi_{0,2}}{r}\right]+5b_2\int\Phi_{0,2}\,dr = s_{0,0}\,r-b_0\int\Phi_{0,0}\,dr-\frac{1}{14b_3}\left[\Phi'_{2,2}+3\int\frac{d\Phi_{2,2}}{r}\right]\\
&-\left[\frac{2}{b_1}+\frac{16}{7b_3}\right]\left[\Phi'_{2,2}+\int\frac{d\Phi_{2,2}}{r}+4\int\Phi_{2,2}\,d\left(\frac{1}{r}\right)\right]+10b_2\int\Phi_{2,2}\,dr\\
&=-\left[\frac{12}{7b_3}+\frac{4}{b_1}\right]\left[\Phi'_{0,2}-\int\frac{d\Phi_{0,2}}{r}\right]+\frac{4}{b_1}\left[\Phi'_{0,0}-\int\frac{d\Phi_{0,0}}{r}\right]
\end{aligned}\right\} \quad (6)$$

The first of equations (6) will hereafter be called the $\Phi_{0,0}$ equation. The second will be called the $\Phi_{0,2}$ equation and the third the $\Phi_{2,2}$ equation.

An identical set of equations holds in region A (see fig. 3), except that $s_{0,0} = 0$ and the terms containing b are replaced by terms containing a.

Boundary conditions. - Referring again to figure 3 the following boundary conditions must hold:

$$F(b,\mu,\alpha) = F(b,-\mu,\alpha+\pi) \qquad \text{at} \quad r = b \qquad (7a)$$

$$F^A(a,\mu,\alpha) = F^B(a,\mu,\alpha) \qquad \text{at} \quad r = a \qquad (7b)$$

$$F(0,\mu,\alpha_1) = F(0,\mu,\alpha_2) \qquad \text{at} \quad r = 0 \qquad (7c)$$

α_1 and α_2 arbitrary

$F(0,\mu,\alpha)$ finite

Equation (7a) is a statement of the fact that no net flow of neutrons occurs across the outer boundary of the cell in any arbitrary direction. Though this condition is strictly true for cylindrical cells with square outer boundaries, it can only be approximately true for cells with circular outer boundaries.

Equation (7b) states that the transport flux in an arbitrary direction at the interface must be continuous across that interface.

Equation (7c) is necessary because at $r = 0$ for a given polar angle the flux must be independent of α. This leads to the same conditions on the $F_{m,n}(r)$ as the requirement $F(0,\mu,\alpha)$ be finite.

Equations (7a) to (7c) lead to the conditions

$$\left.\begin{aligned} F_{1,1}(b) = F_{1,3}(b) = F_{3,3}(b) = 0 \\ F^{A}_{m,n}(a) = F^{B}_{m,n}(a) \\ F_{1,1}(0) = F_{1,3}(0) = F_{3,3}(0) = F_{2,2}(0) = 0 \end{aligned}\right\} m,n=0,1,2,3$$

which imply

$$\Phi'_{0,0} = -5\Phi'_{0,2} \qquad (8a)$$

$$\Phi'_{0,2} = \frac{1}{3}\frac{\Phi_{2,2}}{b} \qquad \text{at} \quad r = b \text{ (outer boundary)} \qquad (8b)$$

$$\Phi'_{2,2} = \frac{2\Phi_{2,2}}{b} \qquad (8c)$$

$$\Phi'_{0,0,A} = \frac{a_1}{b_1}\Phi'_{0,0,B} + \left(\frac{a_1}{b_1} - \frac{a_3}{b_3}\right)\left(\frac{\Phi'_{2,2,B}}{2} - \Phi'_{0,2,B}\right) + \frac{1}{3a}\left(\frac{3a_1}{b_1} + \frac{2a_3}{b_3} - 5\right)\Phi_{2,2,B} \qquad (9a)$$

$$\Phi'_{0,2,A} = \frac{a_3}{b_3}\Phi'_{0,2,B} + \frac{1}{3a}\left(1 - \frac{a_3}{b_3}\right)\Phi_{2,2,B} \qquad (9b)$$

$$\Phi'_{2,2,A} = \frac{a_3}{b_3}\Phi'_{2,2,B} + \frac{2}{a}\left(1 - \frac{a_3}{b_3}\right)\Phi_{2,2,B} \qquad (9c)$$

$$\Phi^A_{0,0} = \Phi^B_{0,0} \qquad \text{at } r = a \text{ (interface)} \qquad (9d)$$

$$\Phi^A_{0,2} = \Phi^B_{0,2} \qquad (9e)$$

$$\Phi^A_{2,2} = \Phi^B_{2,2} \qquad (9f)$$

$$\Phi'_{0,0} = 0 \qquad (10a)$$

$$\Phi'_{0,2} = 0 \qquad (10b)$$

$$\Phi'_{2,2} = 0 \qquad \text{at } r = 0 \text{ (origin)} \qquad (10c)$$

$$\Phi_{2,2} = 0 \qquad (10d)$$

Differential analyzer procedure for solving cylindrical flux equations. - A neutron source of $s_{0,0} = 1$ neutron/(cubic centimeter)(second) is chosen in region B with a zero source in region A. First $\Phi_{0,2}$ and $\Phi_{2,2}$ are set equal to zero in equations (6) to (9), and the resulting cylindrical diffusion equation is solved for $\Phi_{0,0}$.

The diffusion equation for region A and the one for region B are solved in a manner similar to that described in the section Analyzer Procedure for Slab Solutions. This procedure gives the graphical P_2 diffusion theory answer.

Having the P_2 solution, the procedure is to successively solve the $\Phi_{0,2}$, $\Phi_{2,2}$, $\Phi_{0,0}$, $\Phi_{0,2}$, $\Phi_{2,2}$, $\Phi_{0,0}$, and so forth, equations by using the boundary conditions, equations (7) to (9), for the $\Phi_{0,2}$ equation, the third conditions for the $\Phi_{2,2}$ equation, and the first condition for the $\Phi_{0,0}$ equation.

Unlike the rectangular case, inhomogeneous boundary conditions occur at $r = b$, but the solution is still initiated by guessing $\Phi(b)$. The discontinuous change in slope at the interface is calculated by the corresponding Φ equation of equation (8). As in the rectangular case, homogeneous conditions on the slopes of the terms Φ occur at $r = 0$. However, the additional requirement $\Phi_{2,2}(0) = 0$ must also be met.

For the cylindrical case, it was not possible to set the three equations of equation (6) into the analyzer at the same time. Therefore, the following procedure was used:

(1) $\Phi_{2,2}$ is set $\equiv 0$. The $\int \Phi_{0,0} dr$ obtained from the diffusion $\Phi_{0,0}$ equation is fed into the $\Phi_{0,2}$ equation at the proper time. A first approximation $\Phi_{0,2}$ denoted by $\Phi_{0,2}^{(1)}$ is obtained when the value assumed for $\Phi_{0,2}(b)$ leads to $\Phi'_{0,2}(0) = 0$.

(2) The functions $\left(\Phi'_{0,2} - \int \frac{d\Phi_{0,2}}{r}\right)$ obtained from $\Phi_{0,2}^{(1)}$, and $\left(\Phi'_{0,0} - \int \frac{d\Phi_{0,0}}{r}\right)$ obtained from the diffusion $\Phi_{0,0}$ were fed into the $\Phi_{2,2}$ equation. A $\Phi_{2,2}^{(1)}$ is obtained when the $\Phi_{2,2}(b)$ assumed leads to $\Phi'_{2,2}(0) = 0$, and $\Phi_{2,2}(0) = 0$.

(3) The functions $\left(\Phi'_{0,2} + \int \frac{d\Phi_{0,2}}{r}\right)$ obtained from $\Phi_{0,2}^{(1)}$, and $\left(\Phi'_{2,2} + 3\int \frac{d\Phi_{2,2}}{r}\right)$ obtained from $\Phi_{2,2}^{(1)}$ were fed into the $\Phi_{0,0}$ equation. Equation $\Phi_{0,0}^{(1)}$ is obtained when the $\Phi_{0,0}(b)$ assumed leads to $\Phi'_{0,0}(0) = 0$.

(4) The functions $\left(\Phi'_{2,2} + 3\int \frac{d\Phi_{2,2}}{r}\right)$ obtained from $\Phi_{2,2}^{(1)}$ and $\int \Phi_{0,0} dr$ obtained from $\Phi_{0,0}^{(1)}$ were fed into the $\Phi_{0,2}$ equation. The term $\Phi_{0,2}^{(2)}$ is obtained when the $\Phi_{0,2}(b)$ assumed leads to $\Phi'_{0,2}(0) = 0$. Steps 2, 3, and 4 were repeated until the $\Phi_{0,0}$ equation solution produced a neutron conservation of approximately one percent. In solving for $\Phi_{2,2}^{(2)}$ and successive values of $\Phi_{2,2}$, interpolation of the function $\left(\Phi'_{0,2} - \int \frac{d\Phi_{0,2}}{r}\right)$ appearing in the $\Phi_{2,2}$ equation was necessary. The curve to be used for this function had the same shape but it was intermediate between $\left(\Phi'_{0,2} - \int \frac{d\Phi_{0,2}}{r}\right)^{(1)}$ and $\left(\Phi'_{0,2} - \int \frac{d\Phi_{0,2}}{r}\right)^{(2)}$, and between $\left(\Phi'_{0,2} - \int \frac{d\Phi_{0,2}}{r}\right)^{(2)}$ and $\left(\Phi'_{0,2} - \int \frac{d\Phi_{0,2}}{r}\right)^{(3)}$, and so forth. The amount

of interpolation of the function $\left(\Phi'_{0,2} - \int \frac{d\Phi_{0,2}}{r}\right)$ decreased as the error in conservation of the $\Phi_{0,0}$ equation decreased, until the last curve of this function used was practically that obtained from the preceeding $\Phi_{0,2}$ equation. For the two cylindrical problems solved, this procedure required about 40 hours each.

RESULTS AND DISCUSSION

Rectangular Case

The flux distributions for the slab cells studied are shown in figure 2, and table I presents the numerical values of the self-shielding factors. The P_2 approximation differs from the P_3 approximation in calculating self-shielding effects for the examples presented.

The magnitude of self-shielding effects are measured by deviations in R from the value for R_H of 0.712 calculated by assuming a constant flux throughout the cell. For the two-region cell, the deviation from R_H was 0.0107 and 0.0150, respectively, for P_3, unbound and bound, and 0.0048 and 0.0080 for P_2, unbound and bound. For the three-region cell, the deviations were -0.0225 and -0.0224 for P_3, unbound and bound, and -0.0121 for P_2, unbound and bound.

The deviations are positive for the two-region cell because the presence of the source term in the water-uranium region leads to a higher flux and, consequently, more absorption in uranium relative to the case where the flux was constant throughout the slab cell. In the three-region cell, the neutron flux is considerably attenuated by transition through the water and steel regions before absorptions occur in uranium. Hence, a negative deviation from R_H is obtained.

A consideration of chemical binding does not affect values of R for the three-region cell despite an increased flux in water resulting from larger average hydrogen scattering cross sections for the bound cases. The flux is higher in the water region for the bound cases because neutrons undergo more scattering collisions per second which tends to confine them there and build up the flux. This effect is enhanced to some extent by the larger mass number M for the bound case which tends to produce more nearly isotropic scattering that attenuates the streaming of neutrons toward the steel region. Thus a higher R is to be expected for the bound cases. In the two-region cell, chemical binding leads to a larger value of R by virtue of the increased flux in the water-uranium region relative to the unbound case.

Because the total neutron flux is symmetrical about the extreme boundaries of the cell, no leakage occurs from the cell. Thus, for steady state, the total number of neutrons absorbed per second in the cell must equal the total number produced per second. This criterion was applied to each of the flux curves of figure 2 as a check on the accuracy of the analyzer solutions. As can be seen from table I, conservation of neutrons in the slab case is satisfied within about 2 percent for the three-region case and a 1/2 percent for the two-region case; the value of R was found to be insensitive to such small deviations in conservation.

Cylindrical Case

Unbound. - The P_3 approximation $\Phi_{0,0}$ curve and the diffusion $\Phi_{0,0}$ curve shown in figure 5 resulted from solving equations (6) to (9) for the equivalent unbound two-region cylindrical cell problem. The cylindrical P_3 $\Phi_{0,0}$ compares with the P_3 approximation flux $F_0(x)$ for the slab cell in the following manner:

The values of $\Phi_{0,0}$ at the outer boundary, interface, and origin are 1.184, 1.111, and 1.023, respectively, for the cylindrical cell. The corresponding values of F_0 are 1.071, 1.105, and 1.160. The flux in the steel region of the cylinder is lower implying a higher flux in the water-uranium region to satisfy conservation.

Table II gives the results for the cylindrical cell. Unlike table I, the average production and absorption are taken per cubic centimeter-second of material. The average absorption per cubic centimeter-second of region A, for example, is calculated by

$$\frac{\int_{r=0}^{a} \Phi_{0,0}(r)\,dV}{\int_{r=0}^{a} dV} \times \Sigma_A \cong \frac{\left(\sum_i \Phi_{0,0,i}(r_i) r_i \Delta r_i\right) \Sigma_A}{\sum_i r_i \Delta r_i}$$

After calculating the average absorption per cubic centimeter-second in region B, it follows that $R = 0.7198$ for the P_2 approximation and $R = 0.7336$ for the P_3 approximation. Thus, more absorption occurs in the water-uranium region of the cylindrical cell than in the same region of the slab cell.

As in the slab-cell case, conservation of neutrons must be satisfied. The diffusion $\Phi_{0,0}$ and the $P_3\,\Phi_{0,0}$ were approximately 2.0 and 1.2 percent, respectively, too small conservation wise. As for the rectangular case, values of R were found to be insensitive to small deviations in conservation.

Bound case. - The P_2 and P_3 curves for the bound case are shown in figure 6. As was explained for slab cells, a higher flux in the water-uranium region, leading to a larger value of R relative to the unbound case is to be expected when the effects of molecular binding in water are considered. This is verified from table II, where $R = 0.7213$ for P_2 and $R = 0.7355$ for P_3. Conservation is 2 percent and 0.7 percent lacking for these curves.

Values of $\Phi_{0,0}$ at the outer boundary, interface, and origin are 1.200, 1.111, and 1.018, respectively. The corresponding values for $F_0(x)$ in the P_3 approximation for the rectangular cell are 1.060, 1.092, and 1.180, respectively.

CONCLUDING REMARKS

This study shows that the P_3 approximation of transport theory as compared with the diffusion theory approximation gives significant differences for the flux distributions and self-shielding factors of multiregion cells of rectangular and cylindrical geometry. The diffusion approximation underestimated the magnitude of self-shielding effects relative to the P_3 approximation for all cases.

Also, the chemical binding of the hydrogen in the water molecule was found to be important for the two-region cells which considered the uranium to be homogeneously mixed with the water; both the flux distribution and the self-shielding factor were affected. For the three-region cell where the uranium was considered to be a region, the chemical binding effect did not change the self-shielding factor but did alter the flux distributions somewhat.

An electromechanical differential analyzer was found to be suitable for solving the P_2 and P_3 flux equations.

Lewis Flight Propulsion Laboratory
National Advisory Committee for Aeronautics
Cleveland, Ohio, January 17, 1956

APPENDIX A

SYMBOLS

A,B,C	used as either subscripts or superscripts to denote the various regions of a cell
a,b	radii of the cylindrical cell
a_k,b_k,c_k	defined as the difference $(\Sigma - N_S \sigma_{S,k})$
D	the neutron diffusion coefficient defined by $D = \frac{1}{3a_1}$
$F_{j,k}$	the coefficients of the expansion of the flux function in cylindrical geometry
F_k	the k^{th} coefficient of the Legendre expansion of the flux function in rectangular geometry
$F(r,\mu,\alpha)$	definition of the transport flux in cylindrical geometry
H	chemical symbol for hydrogen
$\breve{i},\breve{j},\breve{k}$	unit vectors along x,y,z-axes
k	0,1,2,3
M	atomic mass
N_S	number of scattering nuclei per cubic centimeter of a region
P_n^m	the associated Legendre polynomial of indices n,m
R	self-shielding factor defined as the ratio of absorptions in uranium to the total number of absorptions in a cell
R_H	homogeneous self-shielding factor, $R_H = 0.7120$
r	radial distance from the z-axis
$\breve{r}$	unit radial vector
S	constant isotropic source of thermal neutrons, $\frac{s}{2\pi}$
U	chemical symbol for uranium

V	volume
x	variable distance used for the rectangular cell
$0,\alpha,\beta,\delta$	values of x at the various boundaries of the rectangular cell
α	azimuthal angle of the velocity vector measured from the z-axis
δ	symbol for the Kronecker delta
θ	scattering angle in the laboratory frame of reference
θ_c	scattering angle in the center of mass system
μ	defined by $\mu = \cos \xi$
ν	defined by $\nu = \cos \theta_c$
ξ	polar angle of velocity vector measured from the z-axis
Σ	the total macroscopic neutron cross section
Σ_a	macroscopic neutron absorption cross section
Σ_S	macroscopic neutron scattering cross section
σ_S	microscopic neutron scattering cross section
$\sigma_{S,k}$	the k^{th} coefficient of the Legendre expansion of the scattering function
σ_{tr}	microscopic neutron transport cross section in the laboratory frame of reference
Φ	transport flux
φ	angle between radius vector r and x-axis
ψ	azimuthal angle made by a neutron direction after collision with the neutron direction before collision
$\vec{\Omega}$	unit vector in the direction of neutron velocity

APPENDIX B

THE P_3 APPROXIMATION FOR CYLINDRICAL GEOMETRY

The general steady-state monoenergetic Boltzman transport equation stating the conservation of neutron flux F for an element of volume is (ref. 2)

$$\vec{\Omega} \cdot \nabla F(\vec{r},\vec{\Omega}) + N\sigma(\vec{\Omega})F(r,\vec{\Omega}) = \int_{\vec{\Omega}'} N_S \sigma_S(\vec{\Omega},\vec{\Omega}')F(\vec{r},\vec{\Omega}')d\vec{\Omega}' + S(\vec{r},\vec{\Omega}) \quad (B1)$$

$\vec{\Omega}$ unit vector in the direction of neutron velocity

$d\vec{\Omega}'$ element of solid angle about direction $\vec{\Omega}'$

N number of nuclei per cubic centimeter

N_S number of scattering nuclei per cubic centimeter

σ total microscopic neutron cross section

$N_S\sigma_S(\vec{\Omega},\vec{\Omega}')$ probability per centimeter that a neutron traveling in the direction $\vec{\Omega}'$ undergoes at $\vec{r}$ a scattering collision into a unit solid angle about direction $\vec{\Omega}$

The first term represents the net number of neutrons with direction $\vec{\Omega}$ at $\vec{r}$ leaking out through the faces per cubic centimeter per second. The second term is the loss of neutrons of direction $\vec{\Omega}$ at $\vec{r}$ per cubic centimeter per second due to absorption or scattering collisions. The third term is the number of neutrons per cubic centimeter per second traveling in the direction $\vec{\Omega}'$ that undergoes a scattering collision into the direction $\vec{\Omega}$ at $\vec{r}$. The last term is the number of neutrons produced per cubic centimeter per second with direction $\vec{\Omega}$ at $\vec{r}$.

The following simplifying assumptions are made:

(1) The neutron flux has cylindrical symmetry, that is, F is independent of Φ and z, the spatial azimuthal and axial coordinates for directions of $\vec{\Omega}$ are fixed relative to the direction of $\vec{r}$.

(2) The medium is isotropic, which implies $\sigma(\vec{\Omega}) = \sigma$, a constant, and the scattering is a function only of the angle between the initial direction of the neutron velocity and the final direction.

(3) The scattering is spherically symmetrical in the center of mass system.

Referring to figure 4 in which the direction of the neutron velocity vector at r is given by polar angle ξ and an azimuthal angle α in the plane of the cross section,

$$\vec{\Omega} = \vec{i} \sin\xi \cos(\alpha + \varphi) + \vec{j} \sin\xi \sin(\alpha + \varphi) + \vec{k} \cos\xi$$

$$= \breve{r} \sin\xi \cos\alpha + \breve{\varphi} \sin\xi \sin\alpha + \vec{k} \cos\xi \qquad \text{(B2)}$$

where $\breve{r}$ is a unit radial vector and $\breve{\varphi}$ is a unit vector perpendicular to $\breve{r}$ in the plane of the cross section. Then

$$\vec{\Omega}\cdot\nabla F = \left(\breve{r} \sin\xi \cos\alpha + \breve{\varphi} \sin\xi \sin\alpha + \vec{k} \cos\xi\right) \cdot \left(\breve{r} \frac{\partial F}{\partial r} + \frac{\breve{\varphi}}{r} \frac{\partial F}{\partial \varphi} + \vec{k} \frac{\partial F}{\partial z}\right)$$

$$= \sin\xi \cos\alpha \frac{\partial}{\partial r} F(r,\xi,\alpha) + \frac{1}{r} \sin\xi \sin\alpha \frac{\partial}{\partial \varphi} F(r,\xi,\alpha) +$$

$$\cos\xi \frac{\partial}{\partial z} F(r,\xi,\alpha)$$

In computing $\frac{\sin\xi \sin\alpha}{r} \frac{\partial}{\partial \varphi} F(r,\xi,\alpha)$, $\vec{\Omega}$ must be held fixed as φ changes. (With $\vec{\Omega}$ held fixed, ξ and α do not vary with r, or z, as either variable alone is changed.) This requires that ξ and α be functions of φ despite no explicit dependence of F on φ. Therefore

$$\vec{\Omega}\cdot\nabla F = \sin\xi \cos\alpha \frac{\partial F}{\partial r} + \frac{1}{r} \sin\xi \sin\alpha \left\{\frac{\partial}{\partial \xi} F(r,\xi,\alpha) \frac{\partial \xi}{\partial \varphi} + \frac{\partial}{\partial \alpha} F(r,\xi,\alpha) \frac{\partial \alpha}{\partial \varphi}\right\} \qquad \text{(B3)}$$

since $\cos\xi \frac{\partial}{\partial z} F = 0$.

The condition that $\vec{\Omega}$ remain fixed as φ changes requires that ξ and $\varphi + \alpha$, the angles made by $\vec{\Omega}$ and the fixed z- and x-direction, respectively, be constant so that

$$\left.\begin{aligned} \frac{\partial \xi}{\partial \varphi} &= 0 \\ \frac{\partial \alpha}{\partial \varphi} &= -1 \end{aligned}\right\} \qquad \text{(B4)}$$

Letting $\mu = \cos \xi$, substituting (B4) into (B3) and noting that assumption (2) implies

$$\sigma_S(\vec{\Omega},\vec{\Omega}') = \frac{1}{2\pi} \sigma_S(\mu_0)$$

$$\mu_0 = \cos(\vec{\Omega},\vec{\Omega}') = \cos \xi \cos \xi' + \sin \xi \sin \xi' \cos(\alpha - \alpha')$$

equation (B1) becomes

$$(1 - \mu^2)^{1/2} \left\{\cos \alpha \frac{\partial F}{\partial r} - \frac{\sin \alpha}{r} \frac{\partial F}{\partial \alpha}\right\} + N\sigma F(r,\mu,\alpha) =$$

$$\int_{-1}^{1} \int_{-\pi}^{\pi} \frac{N_S}{2\pi} \sigma_S(\mu_0) F(r,\mu',\alpha') d\alpha' d\mu' + S(r,\mu,\alpha) \qquad \text{(B5)}$$

$\sigma_S(\mu_0)$ is expanded in a series of Legendre polynomials to give

$$\sigma_S(\mu_0) = \sum_{l=0}^{\infty} \frac{2l+1}{2} \sigma_{S,l} P_l(\mu_0)$$

where

$$\sigma_{S,l} = \int_{-1}^{1} \sigma_S(\mu_0) P_l(\mu_0) d\mu_0$$

It is to be noted that $\sigma_{S,0}$ is the total scattering cross section and $\sigma_{S,1}$ is the total scattering cross section times the average cosine of the scattering angle.

By the addition theorem for Legendre polynomials,

$$\frac{N_S \sigma_S}{2\pi} (\mu_0) = \frac{N_S}{2\pi} \left[\sum_{l=0}^{\infty} \frac{2l+1}{2} \sigma_{S,l} P_l(\mu) P_l(\mu') + \right.$$

$$\left. \sum_{l=0}^{\infty} \sum_{M=1}^{l} \frac{(l-M)!}{(l+M)!} (2l+1) \sigma_{S,l} P_l^M(\mu) P_l^M(\mu') \cos M(\alpha - \alpha') \right]$$

which gives the variation of the scattering function in terms of the desired variables. Equation (B5) becomes

$$(1 - \mu^2)^{1/2} \left\{ \cos \alpha \frac{\partial F}{\partial r} - \frac{\sin \alpha}{r} \frac{\partial F}{\partial \alpha} \right\} + N\sigma F(r,\mu,\alpha) = S(r,\mu,\alpha) + \frac{N_S}{2\pi} \int_{-1}^{1} \int_{-\pi}^{\pi} F(r,\mu',\alpha') \left\{ \sum_{l=0}^{\infty} \frac{2l+1}{2} \sigma_{S,l} P_l(\mu) P_l(\mu') + \sum_{l=0}^{\infty} \sum_{M=1}^{l} \frac{(l-M)!}{(l+M)!} (2l+1) \sigma_{S,l} P_l^M(\mu) P_l^M(\mu') \cos M(\alpha - \alpha') \right\} d\alpha' \, d\mu' \qquad (B6)$$

Symmetry demands that

$$\left. \begin{aligned} F(r,\mu,\alpha) &= F(r,\mu,-\alpha) \\ F(r,\mu,\alpha) &= F(r,-\mu,\alpha) \end{aligned} \right\} \qquad (B7)$$

The transport flux is expanded in a set of spherical harmonics to give

$$F(r,\mu,\alpha) = \sum_{n=0}^{\infty} \sum_{m=0}^{\infty} \frac{(n-m)!}{(n+m)!} \frac{2n+1}{2} F_{m,n}(r) \cos m\alpha \, P_n^m(\mu) \qquad F_{m,n} \equiv 0 \quad m > n \qquad (B8)$$

Harmonic terms containing $\sin \alpha$ do not appear in (B8) because of the first of conditions (B7). The second of conditions (B7) implies that $F_{m,n}(r) \equiv 0$ for either subscript even and the other odd since $P_n^m(-\mu) = (-1)^{n+m} P_n^m(\mu)$. In the P_3 approximation, $F_{m,n}(r)$ is neglected when $n > 3$. The function $S(r,\mu,\alpha)$ is likewise expanded in spherical harmonics (for isotropic sources only the $m = 0$ terms are present).

Multiplying both sides of equation (B8) by $\cos j\alpha \, P_k^{(j)}(\mu) d\mu \, d\alpha$ and integrating over all μ and α gives

$$\left(2\pi \delta_{j,0} + \pi \delta_{j \neq 0} \right) F_{j,k}(r) = \int_{-\pi}^{\pi} \int_{-1}^{1} F(r,\mu,\alpha) \cos j\alpha \, P_k^{(j)}(\mu) d\mu \, d\alpha$$

$j,k = 1,2,3$ in the P_3 approximation. The ordinary Kronecker delta $\delta_{m,S}$ is defined as

$$\delta_{m,S} \equiv \begin{cases} 0 & m \neq S \\ 1 & m = S \end{cases}$$

where $\delta_{m\neq S}$ is defined[1] as

$$\delta_{m\neq S} \equiv \begin{cases} 1 & \text{for } m \neq S \\ 0 & \text{for } m = S \end{cases}$$

This relation follows from the orthogonality properties

$$\int_{-\pi}^{\pi} \cos m\alpha \cos j\alpha \, d\alpha = \delta_{m,j}\left(\pi \, \delta_{j\neq 0} + 2\pi \, \delta_{j,0}\right) \equiv \begin{cases} 0 & m \neq j \\ \pi & m = j \neq 0 \\ 2\pi & m = j = 0 \end{cases}$$

$$\int_{-1}^{1} P_n^{(j)}(\mu) P_k^{(j)}(\mu) d\mu = \frac{(n+j)!}{(n-j)!} \frac{2}{2n+1} \delta_{n,k}$$

As is explained in the ANALYSIS section, the total neutron flux $2\pi F_{0,0}(r) = \Phi_{0,0}(r)$; the net neutron current $\pi F_{1,1}(r) = \Phi_{1,1}(r)$; and the total source strength $2\pi S_{0,0} = s_{0,0}$.

Substituting equation (B8) into (B6), multiplying (B6) by $\cos j\alpha \, P_k^j(\mu) \, d\alpha \, d\mu$ and integrating over α from $-\pi$ to π and then integrating over μ from -1 to 1 (over all directions) and after dividing through by 2π

[1] In this appendix, it is particularly convenient to introduce a "modified" delta function notation defined in this way.

$$\sum_{n=0}^{\infty}\sum_{m=0}^{\infty}\frac{(n-m)!}{(n+m)!}\frac{2n+1}{2}\int_{-1}^{1}(1-\mu^2)^{1/2}P_k^{(j)}(\mu)P_n^{(m)}(\mu)d\mu\left\{F'_{m,n}(r)\right.$$

$$\left.\int_{-\pi}^{\pi}\cos\alpha\cos m\alpha\cos j\alpha\,d\alpha+\frac{mF_{m,n}(r)}{r}\int_{-\pi}^{\pi}\sin\alpha\sin m\alpha\cos j\alpha\,d\alpha+\right.$$

$$N\sigma F_{j,k}(r)\left(\delta_{j,0}+\frac{1}{2}\delta_{j\neq0}\right)=S_{j,k}(r)\left(\delta_{j,0}+\frac{1}{2}\delta_{j\neq0}\right)+$$

$$N_S\sigma_{S,k}F_{j,k}(r)\left(\delta_{j,0}+\frac{1}{2}\delta_{j\neq0}\right)$$

Performing the integration over α, the leakage term in the P_3 approximation can be written

$$\frac{1}{4}\sum_{n=0}^{\infty}\frac{(n-m)!}{(m+n)!}\frac{2n+1}{2}\int_{-1}^{1}(1-\mu^2)^{1/2}P_k^{(j)}(\mu)P_n^{(m)}(\mu)d\mu\left\{F'_{m,n}\sum_{p=0}^{1}\delta_{m,p}\delta_{j,1-p}+\right.$$

$$\sum_{p=0}^{3}\delta_{m,p}\left(\delta_{j,p-1}+\delta_{j,p+1}\right)F'_{m,n}+\frac{mF_{m,n}}{r}\sum_{p=0}^{1}\delta_{m,p}\delta_{j,1-p}+$$

$$\left.\sum_{p=0}^{3}\delta_{m,p}\left(\delta_{j,p-1}-\delta_{j,p+1}\right)\frac{mF_{m,n}}{r}\right\}$$

or

$$\sum_{n=0}^{\infty}\sum_{p=0}^{1}\frac{(n-p)!}{(n+p)!}\frac{2n+1}{2}\int_{-1}^{1}(1-\mu^2)^{1/2}P_k^{(1-p)}(\mu)P_n^{p}(\mu)d\mu\left\{F'_{p,n}+\frac{pF_{p,n}}{r}\right\}\frac{1}{4}\delta_{j,1-p}+$$

$$\sum_{n=0}^{\infty}\sum_{p=0}^{3}\frac{(n-p)!}{(n+p)!}\frac{2n+1}{2}\int_{-1}^{1}(1-\mu^2)^{1/2}P_k^{(p-1)}(\mu)P_n^{(p)}(\mu)d\mu\left\{F'_{p,n}+p\frac{F_{p,n}}{r}\right\}\frac{1}{4}\delta_{j,p-1}+$$

$$\sum_{n=0}^{\infty}\sum_{p=0}^{3}\frac{(n-p)!}{(n+p)!}\frac{2n+1}{2}\int_{-1}^{1}(1-\mu^2)^{1/2}P_k^{(p+1)}(\mu)P_n^{(p)}(\mu)d\mu\left\{F'_{p,n}-p\frac{F_{p,n}}{r}\right\}\frac{1}{4}\delta_{j,p+1}$$

where j has positive values only.

After evaluating the remaining integrals in the leakage term (ref. 3, pp. 102 to 104) the Boltzman equation can finally be written

$$\frac{k(k+1)}{4(2k+1)}\left[F'_{0,k-1} - F'_{0,k+1}\right]\delta_{j,1} + \frac{1}{4(2k+1)}\left[F'_{1,k+1} + \frac{F_{1,k+1}}{r} - F'_{1,k-1} - \frac{F_{1,k-1}}{r}\right]\delta_{j,0} +$$

$$\sum_{p=1}^{3}\frac{1}{4(2k+1)}\left[F'_{p,k+1} + \frac{pF_{p,k+1}}{r} - F'_{p,k-1} - \frac{pF_{p,k-1}}{r}\right]\delta_{j,p-1} +$$

$$\sum_{p=0}^{2}\frac{1}{4(2k+1)}\left[(k+p+1)(k+p)\left(F'_{p,k-1} - \frac{pF_{p,k-1}}{r}\right) - (k-p+1)(k-p)\left(F'_{p,k+1} - \frac{pF_{p,k+1}}{r}\right)\right]\delta_{j,p+1} +$$

$$N\sigma F_{j,k}(r)\left(\delta_{j,0} + \frac{1}{2}\delta_{j\neq 0}\right) = N_S\sigma_{S,k}F_{j,k}(r)\left[\delta_{j,0} + \frac{1}{2}\delta_{j\neq 0}\right] + S_{j,k}(r)\left(\delta_{j,0} + \frac{1}{2}\delta_{j\neq 0}\right)$$

In the P_3 approximation, a set of six simultaneous equations in terms of $F_{m,n}(r)$ are generated by letting j and k independently take on the values $0,1,2,3$

$$F_{m,n}(r) \equiv 0 \quad \text{for} \quad \begin{cases} m \text{ or } n < 0 \\ m \text{ or } n > 3 \\ m > n \\ \text{either subscript even and the other odd} \end{cases}$$

Assuming a constant isotropic source of neutrons, the following set of simultaneous equations are generated:

$$F'_{1,1} + \frac{F_{1,1}}{r} + 2b_0F_{0,0} = 2S_{0,0} \tag{B9a}$$

$$F'_{1,3} + \frac{F_{1,3}}{r} - F'_{1,1} - \frac{F_{1,1}}{r} + 10b_2F_{0,2} = 0 \tag{B9b}$$

$$2F'_{0,0} - 2F'_{0,2} + \frac{1}{2}F'_{2,2} + \frac{F_{2,2}}{r} + 3b_1F_{1,1} = 0 \tag{B9c}$$

$$12F'_{0,2} - \frac{1}{2}F'_{2,2} - \frac{F_{2,2}}{r} + 7b_3F_{1,3} = 0 \tag{B9d}$$

$$F'_{3,3} + \frac{3F_{3,3}}{r} + 12\left(F'_{1,1} - \frac{F_{1,1}}{r}\right) - 2\left(F'_{1,3} - \frac{F_{1,3}}{r}\right) + 10b_2F_{2,2} = 0 \tag{B9e}$$

$$15\left(F'_{2,2} - \frac{2F_{2,2}}{r}\right) + 7b_3F_{3,3} = 0 \tag{B9f}$$

where $b_k = N\sigma - N_S\delta_{S,k}$; $k = 0, 1, 2, 3$.

By setting $F_{0,2}$ and $F_{2,2} \equiv 0$ in (B9c), equations (B9a) and (B9c) reduce to the ordinary cylindrical diffusion equation when they are transformed by

$$2\pi F_{0,k} = \Phi_{0,k}$$

$$\pi F_{j,k} = \Phi_{j,k}$$

$$2\pi S_{0,0} = s_{0,0}$$

APPENDIX C

CALCULATION OF COEFFICIENTS IN P_3 APPROXIMATION

NEUTRON FLUX EQUATIONS

The term a_k appearing in equations (1) is given by

$$a_k = \Sigma^A - N_S^A \sigma_{S,k}^A \qquad k=0,1,2,3 \tag{C1}$$

where the superscripts (which will hereafter be dropped) refer to region A. The $\sigma_{S,k}$ appearing in (C1) is the coefficient of the k^{th} Legendre polynomial in the series expansion of the scattering function, that is

$$\sigma_S(\mu_0) = \sum_{l=0}^{\infty} \frac{2l+1}{2} \sigma_{Sl} P_l(\mu_0)$$

By the orthogonality of Legendre polynomials

$$\sigma_{S,k} = \int_{-1}^{1} \sigma_S(\mu_0) P_k(\mu_0) d\mu_0 \tag{C2}$$

The physical meaning of $\sigma_{S,0}$ and $\sigma_{S,1}$ can be deduced from the following considerations:

The term $N_S \sigma_S(\vec{\Omega},\vec{\Omega}')$ is the probability per centimeter that a neutron traveling in the direction $\vec{\Omega}'$ is scattered into the direction $\vec{\Omega}$ from following sketch. Scattering is assumed to depend only on the

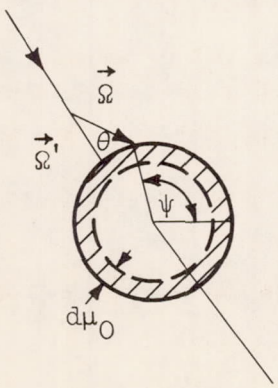

angle θ (or its cosine) where $\vec{\Omega}' \cdot \vec{\Omega} = \cos\theta \equiv \mu_0$. Then a quantity $N_S \sigma_S(\mu_0) d\mu_0$ can be defined as the probability per centimeter of a neutron being scattered from $\vec{\Omega}'$ into an elemental ring of area $2\pi\, d\mu_0$ with direction cosines between μ_0 and $\mu_0 + d\mu_0$. Then

$$N_S d\mu_0 \int_{\psi=0}^{2\pi} \sigma_S(\vec{\Omega}, \vec{\Omega}') d\psi = N_S \sigma_S(\mu_0) d\mu_0$$

or

$$N_S \sigma_S(\vec{\Omega}, \vec{\Omega}') = \frac{N_S}{2\pi} \sigma_S(\mu_0)$$

For $k = 0$, the right side of equation (C2) is the scattering function integrated over all velocity directions so that $\sigma_{S,0}$ is the total microscopic cross section for scattering.

For $k = 1$, $P_1(\mu_0) = \mu_0$ so that $\sigma_{S,1}$ is $\sigma_{S,0}$ times the average cosine $\bar{\mu}_0$ of the scattering angle.

Now

$$\sigma_S(\mu_0) d\mu_0 = p(\mu_0) d\mu_0\, \sigma_{S,0}$$

where $\sigma_{S,0}$ is the probability that a neutron is scattered and $p(\mu_0) d\mu_0$ is the probability that the scattered neutron has the direction cosine μ_0 between μ_0 and $\mu_0 + d\mu_0$. This probability must be independent of the coordinate system, therefore

$$p(\mu_0) d\mu_0 = p(\nu) d\nu$$

where $p(\nu) d\nu$ is the probability of scattering into the angle $2\pi\, d(\cos\theta_c)$ in the center of mass system where θ_c is the scattering angle in the center of mass system and $\nu = \cos\theta_c$.

Assumption of spherically symmetrical scattering in the center of mass system implies

$$p(\nu) d\nu = \frac{2\pi d\nu}{4\pi} = \frac{1}{2} d\nu$$

Therefore,

$$\sigma_S(\mu_0) d\mu_0 = \frac{\sigma_{S,0}}{2} d\nu$$

Applying the laws of conservation of energy and momentum for elastic collision of a neutron with a stationary nucleus of mass M, yields

$$\mu_0 = \frac{M\nu + 1}{(M^2 + 2M\nu + 1)^{1/2}} \tag{C3}$$

which relates the cosine of the scattering angle in the laboratory system to that of the center of mass system. Equation (C2) can then be written

$$\sigma_{S,k} = \int_{-1}^{1} \frac{\sigma_{S,0}}{2} P_k(\mu_0) d\nu \tag{C4}$$

Equation (C3) enables the integral in (C4) to be evaluated for k=0,1,2,3 in a straightforward manner with the results

$$\left.\begin{aligned} \sigma_{S,0} &= \sigma_{S,0} \\ \sigma_{S,1} &= \frac{2}{3M} \sigma_{S,0} \\ \sigma_{S,2} &= \sigma_{S,0} \left\{ \frac{5}{8} - \frac{3M^2}{8} - \frac{3}{32M} (M^2 - 1)^2 \ln \left(\frac{M - 1}{M + 1} \right)^2 \right\} \\ \sigma_{S,3} &= 0 \end{aligned}\right\} \tag{C5}$$

The special case of an infinite atomic mass A_∞ (often assumed for heavy nuclei) gives $\sigma_{S,1} = \sigma_{S,2} = \sigma_{S,3} = 0$ which follows from equation (C5). Scattering is then isotropic in the laboratory system of reference, as well. For light atomic nuclei, the scattering is predominantly forward in the laboratory system.

Equations (C5) enable the calculation of $\sigma_{S,k}$ for the P_3 approximation of transport theory. In particular, the values obtained were used to calculate a_k (eq. (C1)), b_k, and c_k appearing in the flux equations for the regions A, B, and C. Only the hydrogen nuclei of the water region were assumed to have a finite mass number.

REFERENCES

1. Weinberg, Alvin M., and Noderer, L. C.: Theory of Neutron Chain Reactions. AECD-3471, Oak Ridge Nat. Lab., United States Atomic Energy Comm., May 15, 1951.

2. Glasstone, S., and Edlund, M.: The Elements of Nuclear Reactor Theory. D. Van Nostrand Co., Inc., 1952.

3. Margenau, Henry, and Murphy, George Moseley: Mathematics of Physics and Chemistry. D. Van Nostrand Co., Inc., 1943.

TABLE I. - RECTANGULAR GEOMETRY

[Homogeneous value of $R_H = 0.712$.]

	Total production	Total absorption	Total fuel absorption	R	R - 0.712
Self-shielding factors for two-region cells					
Transport theory, P_3					
Unbound	0.1993	0.1987	0.1436	0.7227	0.0107
Bound	.1993	.1993	.1449	.7270	.0150
Diffusion theory, P_2					
Unbound	.1993	.2006	.1438	.7163	.0048
Bound	.1993	.1989	.1432	.7200	.0080
Self-shielding factors for three-region cells					
Transport theory, P_3					
Unbound	0.1993	0.2029	0.1399	0.6895	-0.0225
Bound	.1993	.2039	.1406	.6896	-.0224
Diffusion theory, P_2					
Unbound	.1993	.2006	.1404	.6999	-.0121
Bound	.1993	.2026	.1418	.6999	-.0121

TABLE II. - CYLINDRICAL GEOMETRY

[R_H = 0.712]

	Production per (cc)(sec)	Absorption per (cc)(sec)	Fuel absorption per (cc)(sec)	R	R - 0.712
Self-shielding factors for two-region cell					
Transport theory, P_3					
Unbound	1.000	0.9880	0.7248	0.7336	0.0216
Bound	1.000	.9932	.7305	.7355	.0235
Diffusion theory, P_2					
Unbound	1.000	.9790	.7047	.7198	.0078
Bound	1.000	.9802	.7070	.7213	.0093

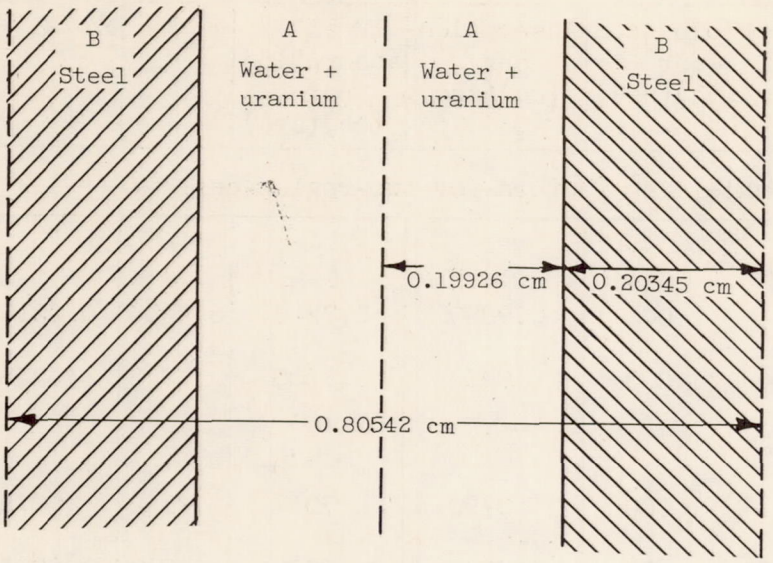

(a) Two-region.

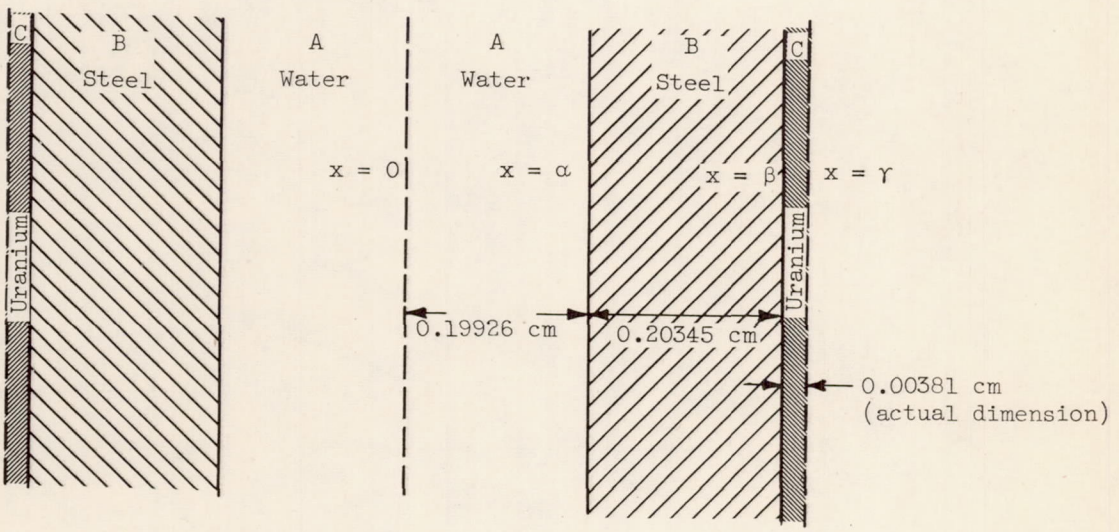

(b) Three-region.

Figure 1. - Rectangular cells.

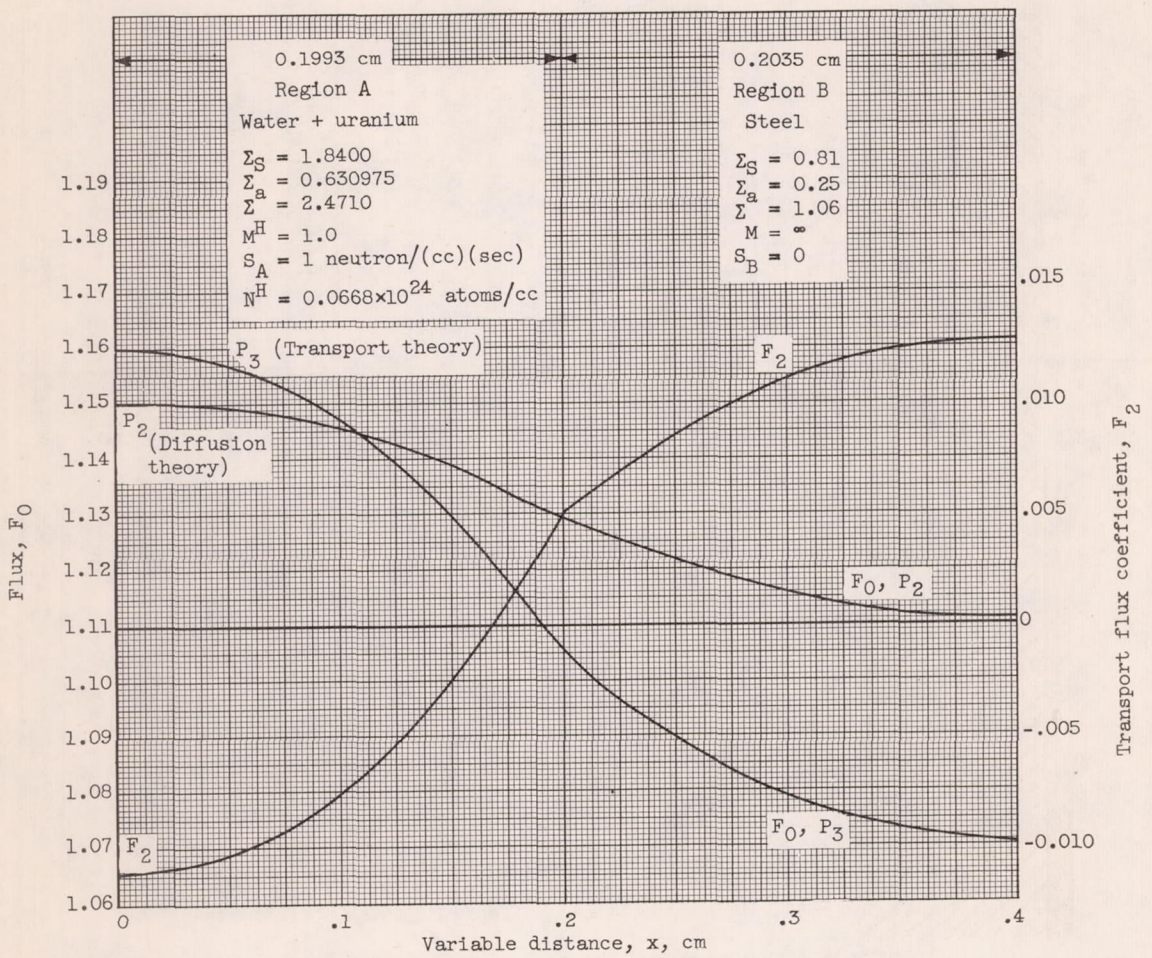

(a) Two-region cell. Molecular binding effects neglected.

Figure 2. - Neutron flux distribution.

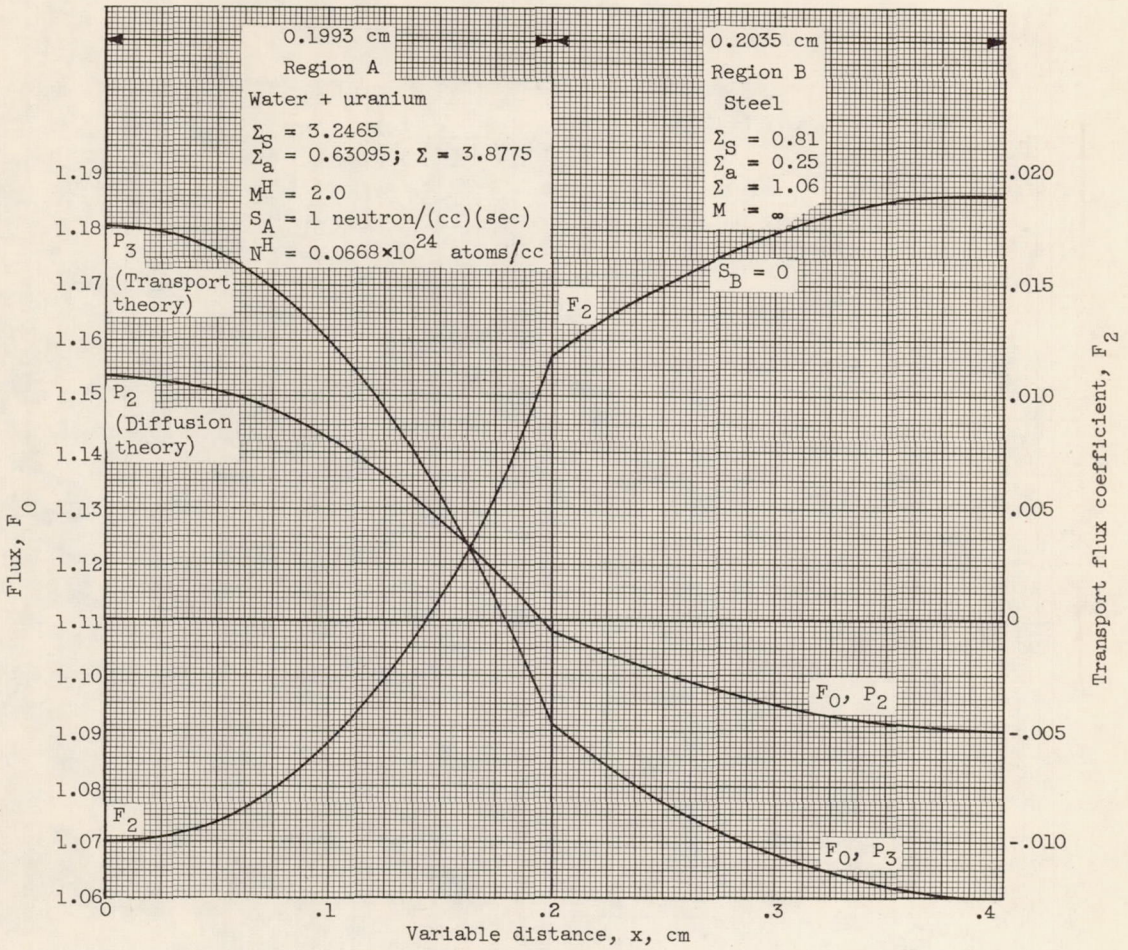

(b) Two-region cell. Molecular binding effects of water approximated.

Figure 2. - Continued. Neutron flux distribution.

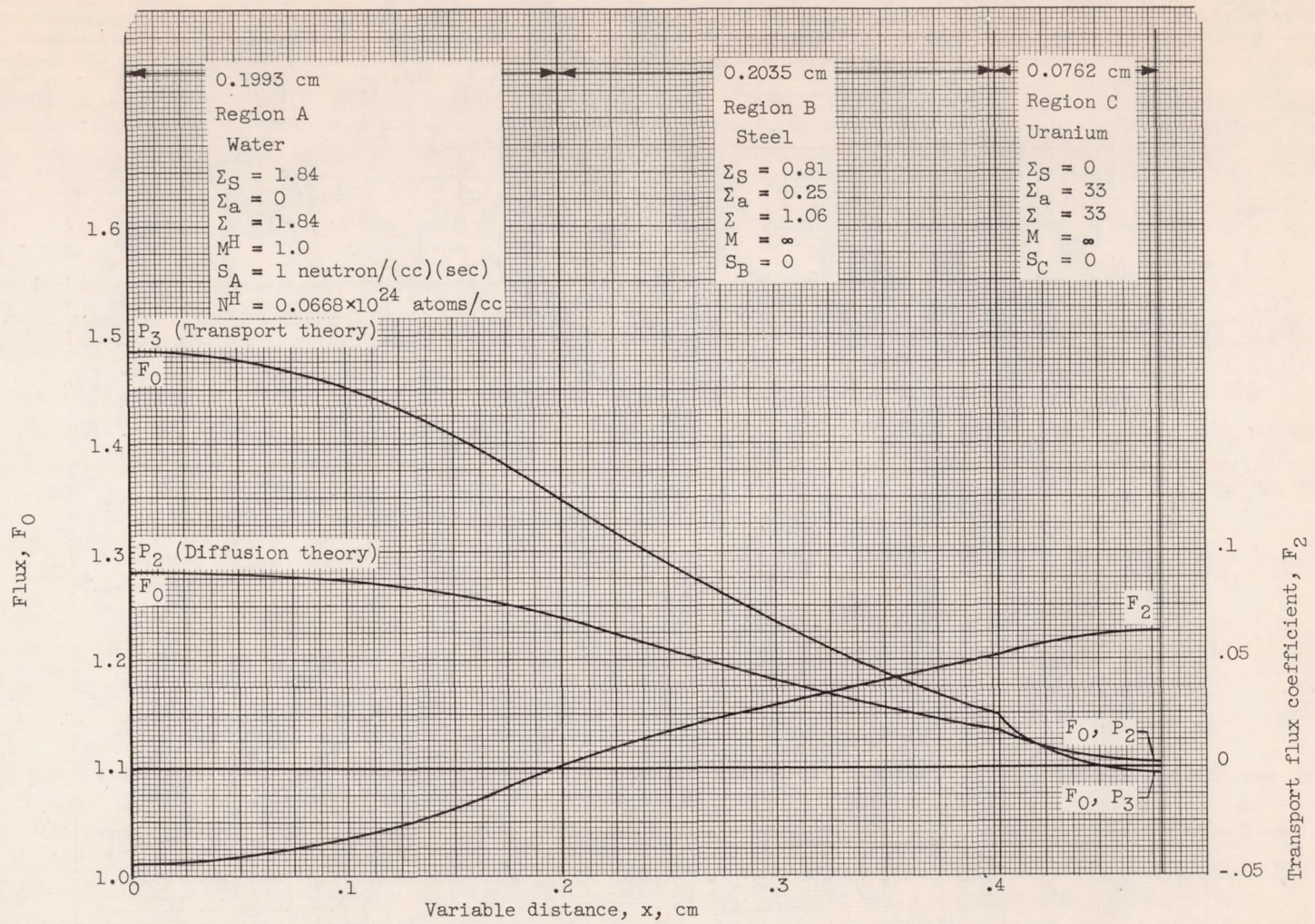

(c) Three-region cell. Molecular binding effects neglected; uranium region shown magnified 20 times.

Figure 2. - Continued. Neutron flux distribution.

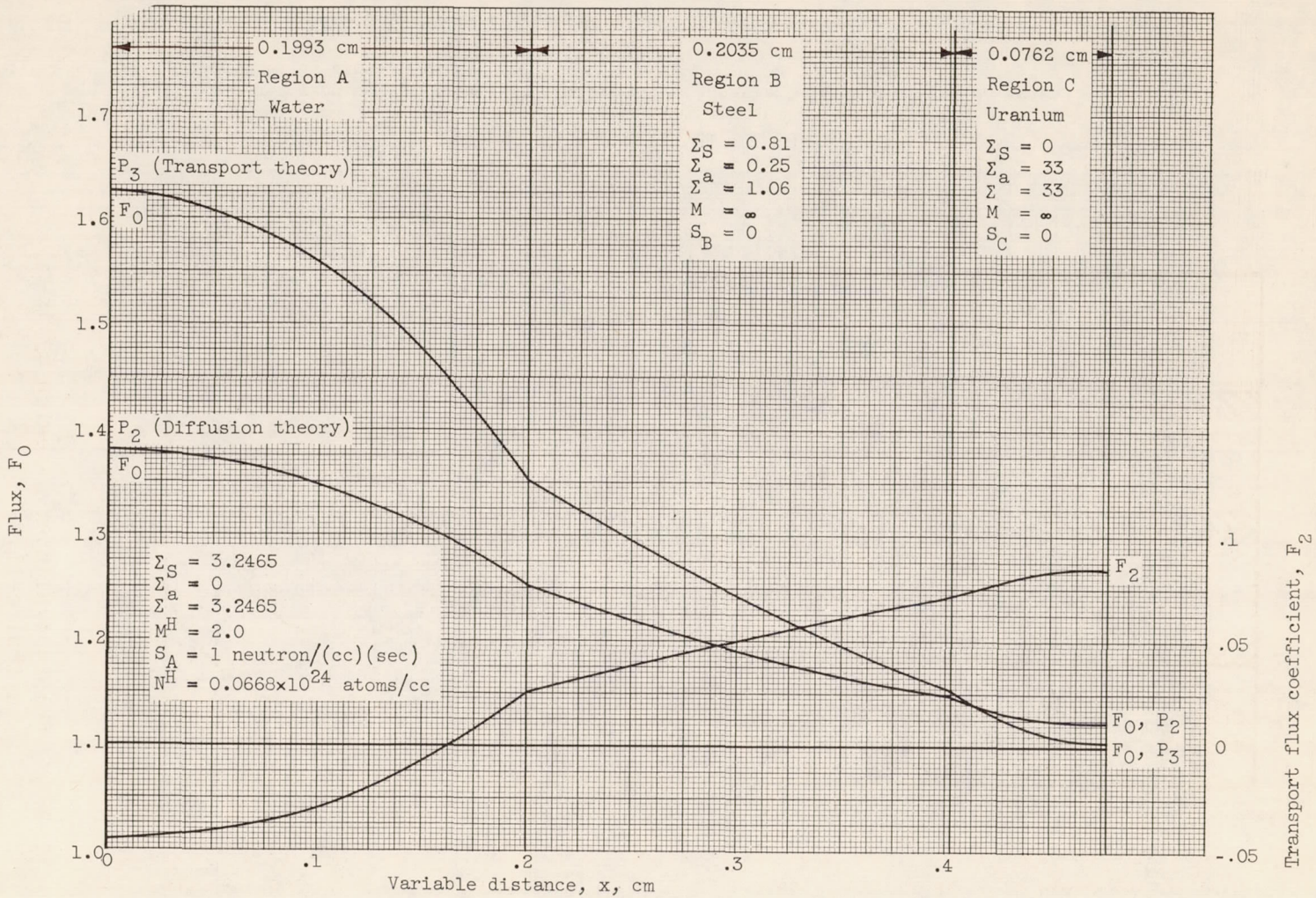

(d) Three-region cell. Molecular binding effect of water approximated; uranium region shown magnified 20 times.

Figure 2. - Concluded. Neutron flux distribution.

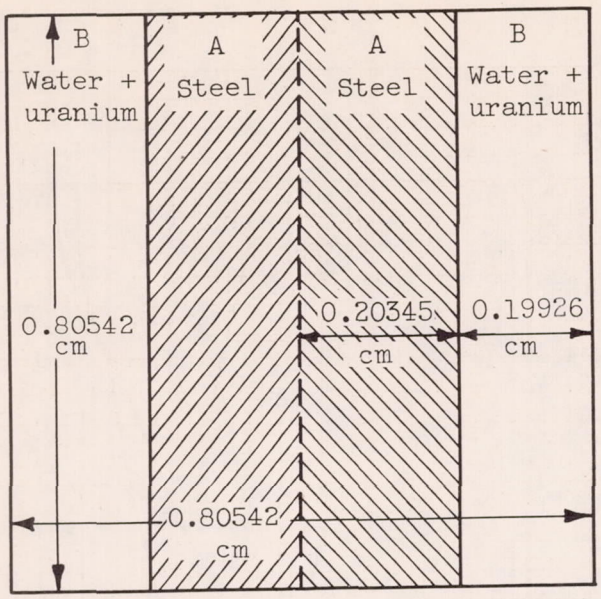

(a) Used to obtain equivalent two-region cylindrical cell.

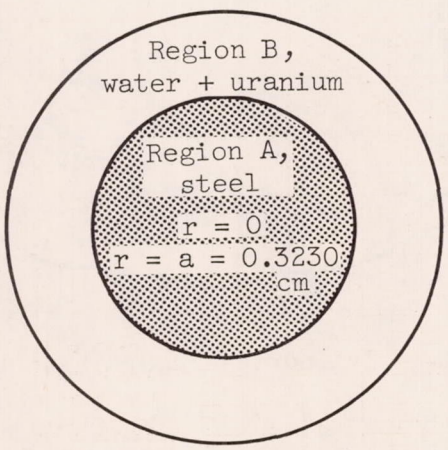

r = b = 0.4544 cm

(b) Equivalent two-region cylindrical cell.

Figure 3. - The cylindrical cell.

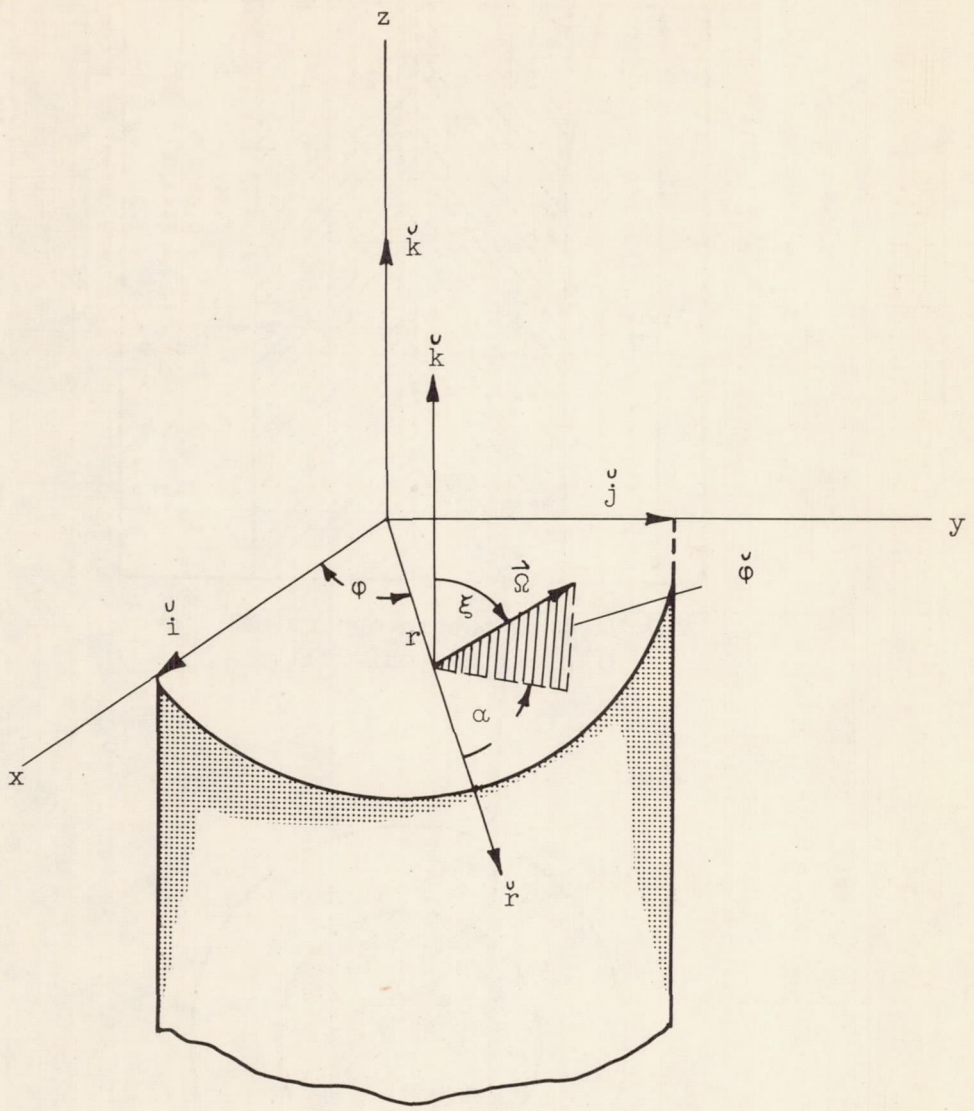

Figure 4. - Cylindrical coordinate system.

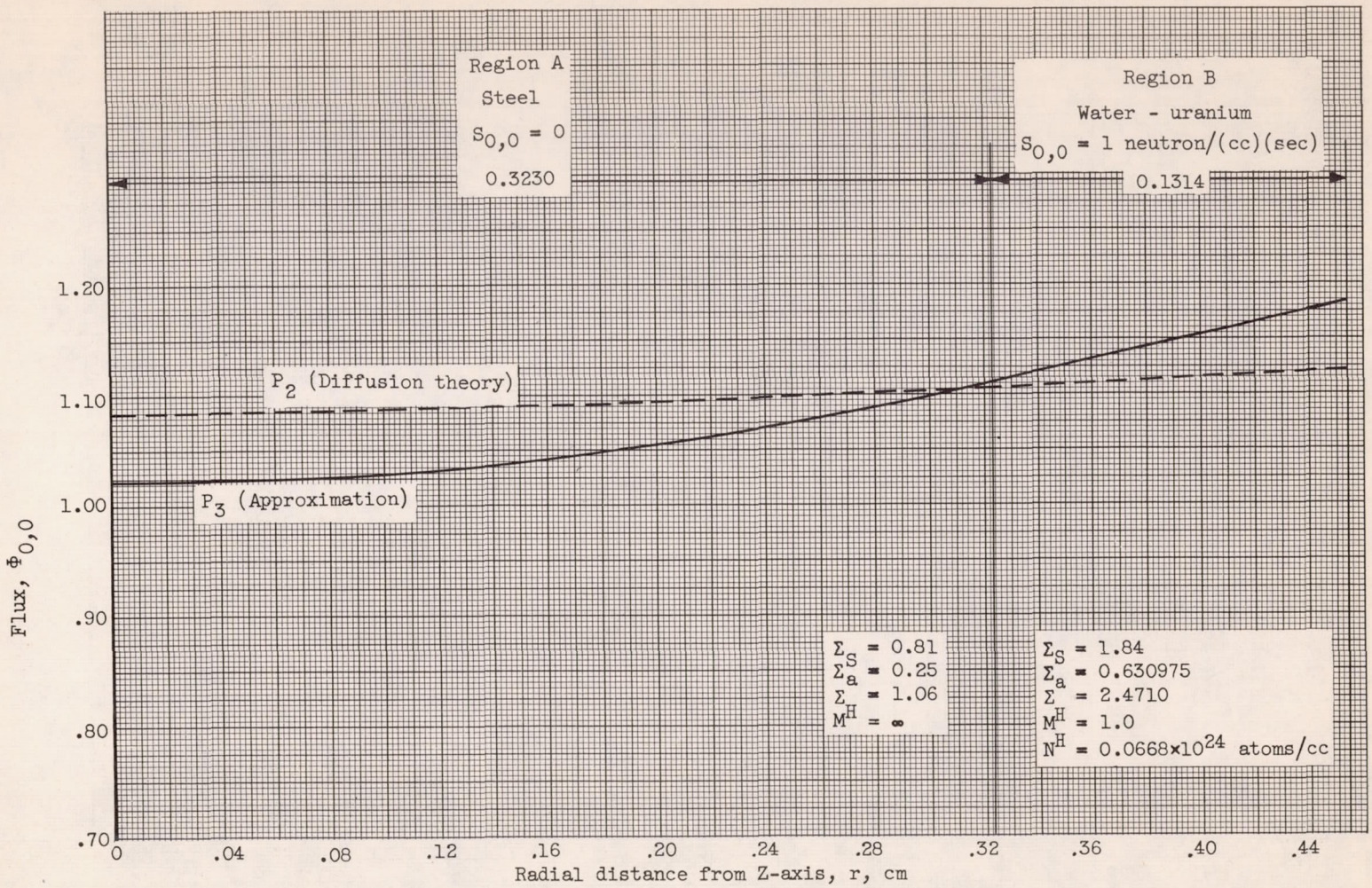

Figure 5. - The unbound two-region cylindrical cell having same homogeneous self-shielding factor as slab cell (0.712).

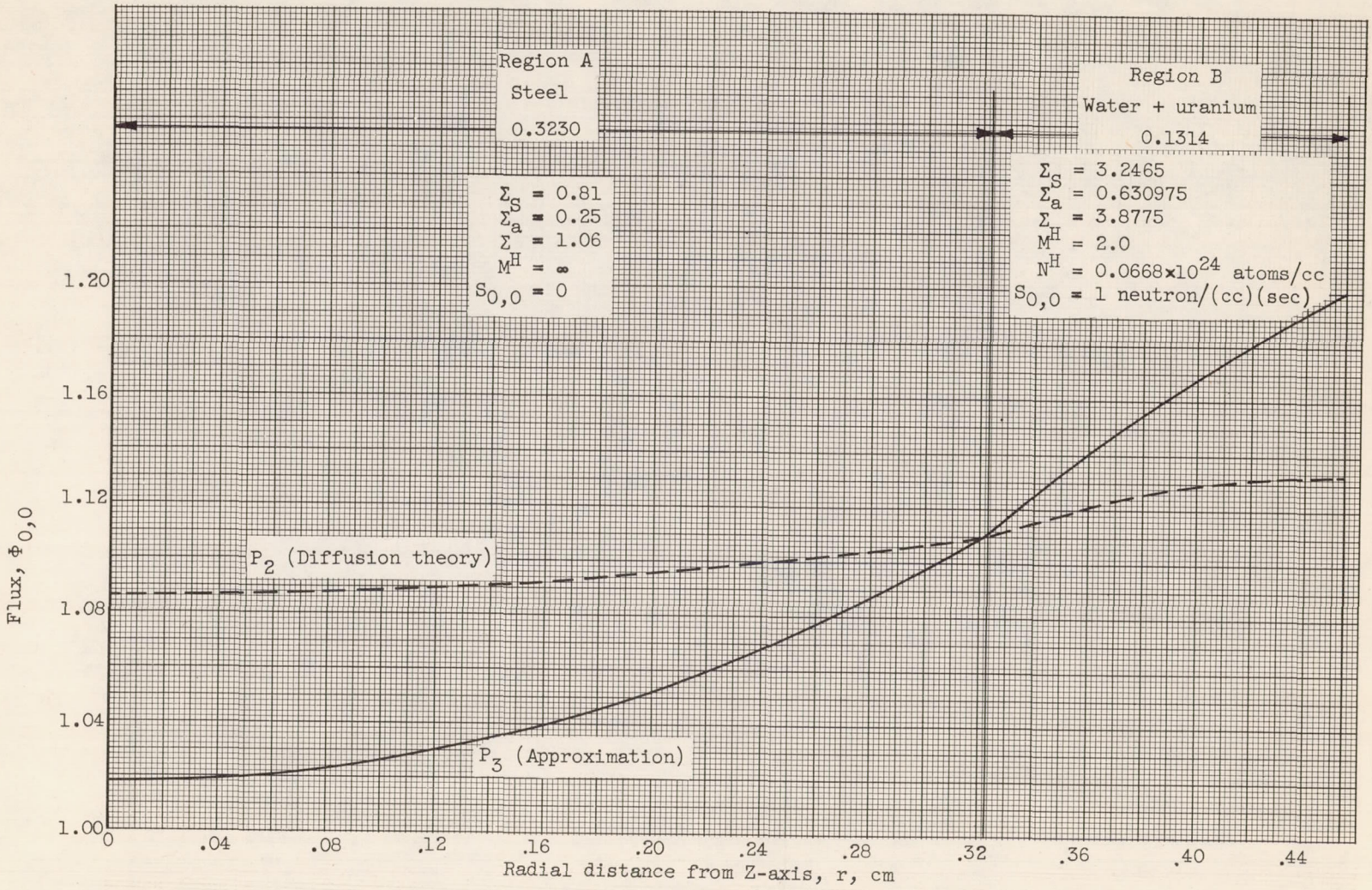

Figure 6. - The bound two-region cylindrical cell having same homogeneous self-shielding factor as slab cell (0.712).